Letters

Synchronous Impedance Spectroscopy Extraction From Reconfigurable Lithium-Ion Battery System via Switching Transient Signal

Jichang Peng, Wen Xie, Jinhao Meng, *Senior Member, IEEE*, and Haitao Liu

***Abstract*—Cell inconsistency in large-scale energy storage system constitutes a critical bottleneck limiting operational efficiency. Reconfigurable battery systems (RBSs) can regulate cell interconnections within modules to achieve cell balance and optimize module performance. However, the control strategies of the RBS depend on precise states of the cells, where conventional current, voltage, and temperature measurement systems inadequately support. This letter proposes an online electrochemical impedance spectroscopy (EIS) measurement method that leverages switching transients during operation of the RBS. An energy-focused S-Transform is introduced to enhance high-frequency impedance acquisition capabilities during transient periods, and thus expanding the bandwidth for EIS. The proposed algorithm achieves precise extraction of cell-level EIS signals from switching transients inherent in RBS reconfiguration, enabling real-time electrochemical state assessment that directly supports advanced RBS control strategies. The validation of the proposed method is proved across a wide temperature range (−20 °C to 35 °C) and multiple states of charge.**

***Index Terms*—Battery energy storage systems (BESSs), electrochemical impedance spectroscopy (EIS), reconfigurable technology, S-transform.**

I. Introduction

THE rapid development of renewable energy sources have catalyzed a broad spectrum of applications for lithium-ion battery energy storage systems (BESSs). These applications include pivotal grid functions, such as peak shaving, voltage and frequency regulation, and inertia support [1]. In such highly dynamic and long-cycle applications, variations in consistency among individual cells within a BESS represent a primary driver of both degradation and safety concerns. Consequently, advancing cell consistency and augmenting energy efficiency within battery packs [2] has emerged as a key for ongoing development of BESS.

Received 19 May 2025; revised 1 July 2025 and 31 July 2025; accepted 15 August 2025. Date of publication 19 August 2025; date of current version 22 October 2025. This work was supported by the National Natural Science Foundation of China under Grant 52477222. *(Corresponding authors: Jichang Peng; Jinhao Meng.)*

Jichang Peng, Wen Xie, and Haitao Liu are with the School of Electric Power Engineering, Nanjing Institute of Technology, Nanjing 211167, China (e-mail: pengjichang@njit.edu.cn; y00450230534@njit.edu.cn; lht@njit.edu.cn).

Jinhao Meng is with the School of Electrical Engineering, Xi'an Jiaotong University, Xi'an 710049, China (e-mail: jinhao@xjtu.edu.cn).

Color versions of one or more figures in this article are available at https://doi.org/10.1109/TPEL.2025.3600334.

Digital Object Identifier 10.1109/TPEL.2025.3600334

Conventional equalization techniques typically transfer energy through capacitors, inductors, and resistors [3]. However, these methods often exhibit limited equalization efficiency and are susceptible to introducing parasitic circulating currents among cells, resulting in substantial energy losses. To overcome the above drawbacks, a reconfigurable battery system (RBS) has been proposed in [4], utilizing the power semiconductor switches to dynamically optimize cell interconnections. This topology aims to enhance both energy efficiency, offering superior balancing performance and greater control flexibility relative to traditional approaches. Consequently, RBS can effectively mitigate cell-to-cell variations and improve overall system reliability. Nevertheless, the design of control strategies and the requirement for accurate battery states remain critical factors that significantly influence the operation of such reconfigurable systems [5].

Currently, control strategies for reconfigurable batteries predominantly utilize temperature [6] and state of charge (SOC) [7] as indicators. However, the accurate acquisition of critical parameters, such as internal temperature, SOC, state of health (SOH), and state of power (SOP) poses considerable challenges in practical RBS, particularly in high-dynamic conditions. Furthermore, these parameters often exhibit significant interdependencies, complicating the optimal reconfiguration when targeting a singular equilibrium objective. Thus, limitations in advanced battery state monitoring and the optimization of reconfiguration strategies can compromise the operational efficacy of these reconfigurable systems.

Electrochemical impedance spectroscopy (EIS) facilitates the characterization of multiscale electrochemical kinetic processes within lithium-ion batteries (LIBs), representing a superior solution for quantifying battery states, such as SOC [8] and internal temperature [9]. Although EIS can effectively reflect the internal states of LIBs, significant challenges persist regarding accurate online impedance acquisition within RBSs. For instance, Chen et al. [10] measured the EIS of RBSs using a multisine excitation signal, which needs specialized control design and additional pulsewidth modulation strategy for the overall system.

However, the injection of multisine signals into highly dynamic RBSs presents considerable challenges for control and can potentially interfere with regular system operation. Conversely, the transient voltage and current profiles generated during the connection and disconnection of individual cells

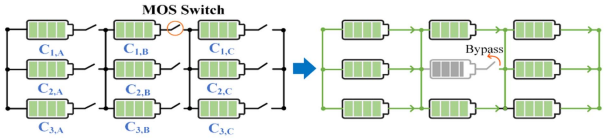

Fig. 1. Reconfigurable battery system.

within the RBS inherently exhibit rich multifrequency content. By applying appropriate frequency analysis methods to these inherent transient features, cell-level EIS detection becomes achievable using only the RBS's existing hardware without requiring additional sensors or external design modifications. It is expected to substantially enhance the state monitoring capabilities of RBSs with minimal additional burden. Therefore, improvements in both state estimation and the fault-tolerant balancing performance of RBSs across diverse operational scenarios can be achieved.

This letter proposes a novel transient step-synchronized EIS measurement solution for RBSs. The main contributions are as follows:

1) A nonintrusive passive EIS detection technology for RBS systems utilizes inherent switching transients, eliminating external excitation requirements.
2) Energy-focused S-Transform (EFST) is introduced to improve the precision of EIS measurement in high-frequency range, thereby expanding the bandwidth of EIS measurement during RBS operation.
3) A 3 × 3 RBS with deep battery state perception capability was designed and validated.

II. Method

A. Reconfigurable Topology

This work presents an RBS architecture featuring cell bypass control, as illustrated in Fig. 1. The proposed system comprises a 3 × 3 cell matrix, where each cell is connected in series with a MOSFET switch. This configuration allows for the flexible connection and disconnection of individual cells by dynamically controlling the conduction states of the MOSFETs with the reconfiguration strategy. The reconfigurable topology provides significant advantages by enabling dynamic management of off-nominal cells, including those with low SOC, temperature anomalies, or aging-related degradation. Through selective bypassing and isolation capabilities, the system maintains equalization efficiency across reconfiguration cycles while ensuring continued operation despite individual cell performance deviations.

B. Reconfiguration Strategy and Transient Analysis

A time-sequence-based reconfiguration strategy is proposed that sequentially bypasses cells at equal time intervals. During reconfiguration cycles, the system simultaneously bypasses target cells while reconnecting previously bypassed one, ensuring stable, continuous battery pack output with minimal fluctuation. Within the control cycle, the output voltage and current of the reconfigurable system can be expressed as

$$V_{\text{out}} = V_{C_{n,A}} + V_{C_{n,B}} + V_{C_{n,C}},\ n \in \{1,2,3\} \tag{1}$$

$$I_{\text{out}} = \frac{V_{\text{out}}}{R_{\text{load}}} \tag{2}$$

$$\begin{cases} I_{\text{cell}} = \frac{I_{\text{out}}}{3} & \text{cell} \in \{\text{PBM } in\ normal\ operation\} \\ I_{\text{cell}} = \frac{I_{\text{out}}}{2} & \text{cell} \in \{\text{PBM } in\ bypassed\ operation\} \end{cases} \tag{3}$$

where V_{out} *and* I_{out} are the voltage and current of the RBS, respectively, and R_{load} is the load resistance. $V_{C_{n,A}}$, $V_{C_{n,B}}$, and $V_{C_{n,C}}$ are the voltages of the three parallel battery modules (PBM). I_{cell} and $V_{\text{cell}}$are the currents and voltages of the battery cells, respectively.

Within a reconfiguration control cycle, a cell previously in bypass mode can be reconnected to the RBS. The resulting voltage and current transients of this cell can be approximated as step signals

$$\begin{cases} V(t) = v_{\text{dc}} + \sum_{k=1}^{N} v_k \cos(n_k \omega_0 t + \phi_k^V) \\ I(t) = i_{\text{dc}} + \sum_{k=1}^{N} i_k \cos(n_k \omega_0 t + \phi_k^I) \end{cases} \tag{4}$$

where v_{dc} and i_{dc} are the dc components, v_k and i_k are the kth harmonic amplitudes, n_k is the harmonic frequency, ω_0 is the fundamental frequency, and ϕ_k^V and ϕ_k^I are the harmonic phase angles.

In this scenario, the battery's voltage is influenced by multitimescale electrochemical reactions, leading to a slow transient decay. Compared to an ideal step signal, the high-frequency components of this voltage transient exhibit accelerated attenuation as frequency increases. The decay law governing the amplitude of these high-frequency components is given by

$$v_k = \frac{2\Delta V}{n_k \pi} \cdot \frac{1}{\sqrt{1 + (n_k \omega_0 \tau_\nu)^2}} \tag{5}$$

where ΔV is the amplitude of the step voltage.

Consequently, the transient responses during reconfiguration are rich in multifrequency content, making them suitable for EIS analysis. However, spectral amplitude attenuation at higher frequencies, particularly in voltage measurements, leads to low signal-to-noise ratios and challenges accurate impedance estimation in the high-frequency range.

C. Impedance Measurement

The S-transform is one of the most effective methods in signal processing for analyzing harmonic components of step signals, offering high harmonic identification accuracy and computational efficiency. In this work, EFST is proposed to enhance the impedance extraction through energy focusing techniques. The proposed EFST optimizes Gaussian window width parameters according to reconstructed switching transient energy spectrum characteristics, significantly improving measurement capability for high-frequency low-amplitude harmonic components. The framework of the designed impedance extraction method is illustrated in Fig. 2.

EFST first calculates the energy distribution $E(f)$ of acquired signals across different frequencies, and then identifies low-energy regions in the spectrum defined as frequency bands

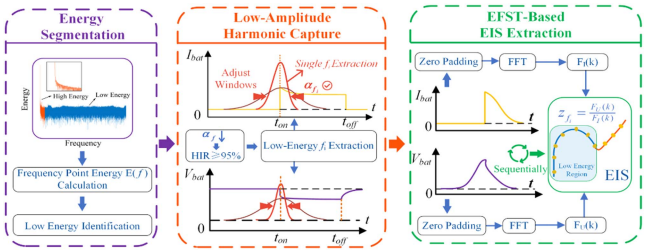

Fig. 2. EIS extraction with EFST.

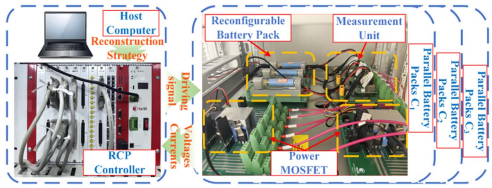

Fig. 3. Experimental platform.

with less than 10% of the maximum energy. The EFST applies adaptive windowing by using varied Gaussian window widths based on these energy characteristics. Specifically, narrower windows are employed in low-energy bands to enhance frequency resolution and enable the detection of subtle variations, which is particularly beneficial for analyzing the characteristics of medium and high-frequency components. Conversely, for high-energy bands exhibiting slower spectral variations, wider windows are utilized to improve frequency resolution, thereby enhancing the accuracy of low-frequency impedance extraction.

The S-transform is defined by (6), where x_N denotes a discrete signal, f represents the frequency, and $g(m-n,f)$ corresponds to the frequency-modulated Gaussian window function given by (7). The standard deviation of this window function is defined in (8), wherein σ is adaptively varied as a function of frequency, determined by the energy distribution and spectral characteristics of the acquired signal

$$S(n,f) = \sum_{m=-\infty}^{+\infty} x_N \cdot g(m-n,f)\, e^{-j2\pi fm} \tag{6}$$

$$g(m-n,f) = \frac{1}{\sqrt{2\pi\sigma^2}}\, e^{-\frac{(m-n)^2}{2\sigma^2}} \tag{7}$$

$$\sigma = \frac{1}{f} \tag{8}$$

$$g(m-n,f) = \frac{1}{\sqrt{2\pi\sigma^2}}\, e^{-\frac{(m-n)^2}{2\sigma^2}} \cdot (\alpha_f). \tag{9}$$

Equation (9) defines the energy-focused adjustment applied to the S-transform Gaussian window function. Within EFST, a dynamic factor α_f is introduced to achieve energy focusing, particularly for high-frequency components in low-energy spectral regions. In these low-energy intervals, α_f is reduced to enhance harmonic identification capability, aligning with the requirements for accurate harmonic analysis. Full-band harmonic information for subsequent impedance estimation is considered available once the harmonic identification rate (HIR) meets the target threshold ($\text{HIR}_{\text{tgt}} \geq 95\%$). HIR_{tgt} is computed using (10), where N_{idt} is the number of successfully identified harmonics, and N_{tgt} is the number of harmonics required to adequately cover the target bandwidth for impedance estimation in low-energy bands

$$\text{HIR}_{\text{tgt}} = \frac{N_{\text{idt}}}{N_{\text{tgt}}} \times 100\%. \tag{10}$$

EFST is obtained by performing the S-transform using the improved window as shown in the following:

$$S_{EF} = \sum_{m=-\infty}^{+\infty} x_N \cdot g(m-n,f) \cdot \alpha_f e^{-j2\pi fm}. \tag{11}$$

When the sampling frequency is f, the discrete signals u_N and i_N with signal length N, and N_τ as the starting point after executing the EFST on the acquired voltage and current can be used to calculate the EIS as

$$Z(k,f) = \frac{\sum_{n=N_\tau-\frac{N}{2}}^{N_\tau+\frac{N}{2}-1} u_N \cdot g(N-N_\tau,f) \cdot \alpha_f e^{-j2\pi kn}}{\sum_{n=N_\tau-\frac{N}{2}}^{N_\tau+\frac{N}{2}-1} i_N \cdot g(N-N_\tau,f) \cdot \alpha_f e^{-j2\pi kn}}. \tag{12}$$

III. Experimental Validation

A. Experimental Testbench

The experimental platform developed for this work is an RBS consisting of nine ICR-18650-15P cells (1.5 Ah, 2.5–4.2 V, −20 °C to 60 °C), as shown in Fig. 3. Each cell channel features a MOSFET switch and integrated voltage/current acquisition circuitry. The system is controlled by a host computer interfaced with an rapid control prototyping (RCP) controller. To cover the EIS detection range for multiple electrochemical battery types, the impedance detection bandwidth was set to 0.2–2000 Hz, capturing key electrochemical processes, with a reconfiguration period of 25 s and a sampling frequency of 10 kHz. The method presented in this letter enables online EIS detection of RBS systems without requiring specialized EIS detection hardware or EIS excitation circuits.

B. Reconfiguration Strategy

This subsection validates the RBS reconfiguration control strategy. Fig. 4 illustrates the voltage and current profiles for each cell and the total RBS current during dynamic reconfiguration operations. The validation algorithm demonstrates full-frequency EIS extraction capability during a stable 25 s switching period, while high-speed dynamic scenarios remain outside this study's scope. Specifically, Fig. 4(a)–(c) demonstrates the voltage and current during sequential battery switching at uniform intervals, highlighting the capability of the RBS to accurately capture voltage and current step transients during the reconfiguration process. The parameter T_{on} represents the initiation point of voltage and current step responses when previously inactive cells connect to the reconfigurable system.

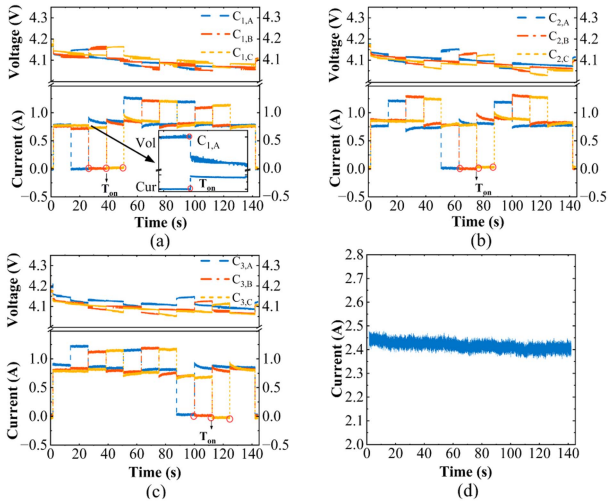

Fig. 4. Experimental results for the RBS reconfiguration. (a) C1,A– C1,C. (b) C2,A– C2,C. (c) C3,A– C3,C. (d) Total current.

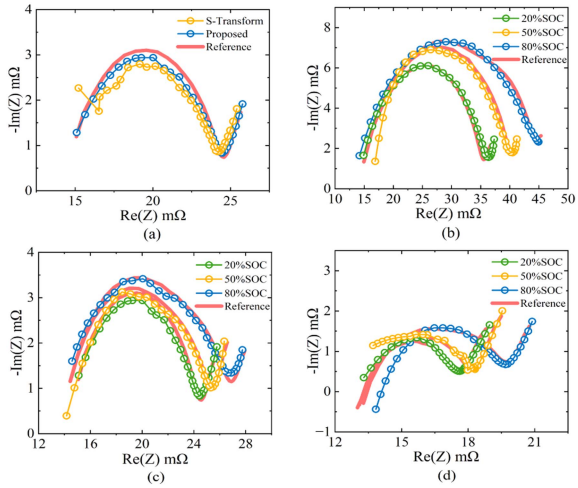

Fig. 5. EIS measurements during the reconfiguration process. (a) 80% SOC at 25 °C, (b) 15 °C, (c) 25 °C, and (d) 35 °C.

The battery connection transient current exhibits a distinct step response, while the voltage transient demonstrates multitimescale gradual decay. These experimental waveforms, reflecting the dynamic characteristics of battery switching, serve as the foundation for wideband EIS estimation based on transient switching responses.

Fig. 4(d) shows a nearly constant current during battery switching, validating the capability of the platform to adjust cell configurations while maintaining uninterrupted power delivery.

C. Impedance Measurement

This section presents EIS test performed at 25 °C and 80% SOC utilizing the reconfiguration transient step. Results obtained using the proposed method are compared with those from the conventional S-transform. Fig. 5(a) shows the EIS measured by both methods. While the two approaches demonstrated good accuracy in the low-frequency range, the proposed method, by dynamically adjusting the Gaussian window, achieved an RMSE

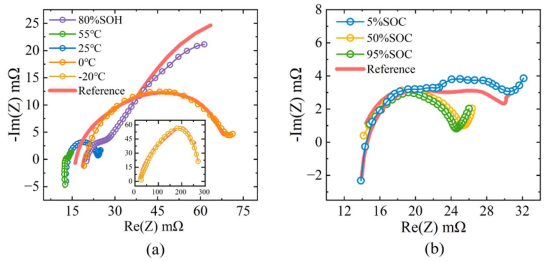

Fig. 6. Results for abnormal cells. (a) −20 °C, 0 °C, 55 °C and 80% SOH. (b) Impedance measured at 5% and 95% SOC.

of 4.8×10^{-4} Ω (real part) and 1.7×10^{-4} Ω (imaginary part). This represents a significant improvement over the conventional S-transform, with RMSE errors reduced by 13.3% and 41.7% for the real and imaginary parts, respectively.

To verify the applicability of the proposed method, nine sets of EIS experiments based on reconfiguration transients are conducted across varying operating conditions (20%, 50%, and 80% SOC, and 15 °C, 25 °C, and 35 °C), as shown in Fig. 5(b)–(d). The experimental results demonstrate that the proposed method achieves good agreement with the reference EIS over the full frequency range under all nine distinct conditions. This confirms that the method can stably measure the battery EIS under various conditions, with the error consistently remaining within 10%.

To validate the proposed method's capability in characterizing anomalous cells within RBS, EIS tests are performed on cells under abnormal conditions. Fig. 6(a) presents EIS for cells subjected to elevated temperature (−20 °C, 0 °C, and 55 °C) and degradation (80% SOH and 1.2 Ah). Fig. 6(b) shows the EIS extraction results at extreme SOC points (5% and 95%). The results indicate that EIS error is slightly higher at extremely low SOC, reaching 11.47%. This error occurs due to insufficient step excitation energy in the high-impedance low-frequency range. Overall, these results confirm the potential of the proposed method in detecting anomalous states, thereby supporting enhanced reconfiguration strategy optimization.

IV. Conclusion

This letter presents an RBS with integrated EIS measurement capability using an EFST-based enhancement method for reconfigurable switching transients. Experimental validation confirms the accuracy of the proposed method and its applicability under multiple conditions. The method demonstrates comprehensive compatibility with mainstream lithium-ion batteries of different cathode chemistries, various aging states, and reconfigurable topological structures. Since the reconfiguration process does not introduce additional detection devices or excitation steps, the proposed method does not impact the efficiency of the reconfiguration system or the lifespan of the battery cells.

The RBSs can maintain stable power during dynamic reconfiguration of cell, while simultaneously performing impedance measurements. This strategy captures the full-spectrum EIS, achieving impedance RMSE less than 0.99 mΩ (real part) and 0.585 mΩ (imaginary part), with particularly enhanced precision in the high-frequency range.

Future work will build upon the EIS-enabled RBS to develop advanced battery state estimation and dynamic reconfiguration strategies, as well as algorithm deployment and efficiency enhancement in commercial large-scale multicell RBS systems.

REFERENCES

[1] Y. Dai, Q. Peng, T. Liu, J. Meng, F. Gao, and F. Blaabjerg, "Negative resistor-based equivalent circuit model of lithium-ion battery energy storage system for grid inertia support," *IEEE Trans. Power Electron.*, vol. 39, no. 11, pp. 15217–15230, Nov. 2024, doi: 10.1109/TPEL.2024.3437176.

[2] M. Koseoglou, E. Tsioumas, N. Jabbour, and C. Mademlis, "Highly effective cell equalization in a lithium-ion battery management system," *IEEE Trans. Power Electron.*, vol. 35, no. 2, pp. 2088–2099, Feb. 2020, doi: 10.1109/TPEL.2019.2920728.

[3] G. D. Astudillo, H. Beiranvand, F. Cecati, C. Werlich, A. Würsig, and M. Liserre, "Integrated strategy for optimized charging and balancing of lithium-ion battery packs," *IEEE Trans. Transport. Electrific.*, vol. 11, no. 1, pp. 4980–4991, Feb. 2025, doi: 10.1109/TTE.2024.3473989.

[4] W. Han, T. Wik, A. Kersten, G. Dong, and C. Zou, "Next-generation battery management systems: Dynamic reconfiguration," *IEEE Ind. Electron. Mag.*, vol. 14, no. 4, pp. 20–31, Dec. 2020, doi: 10.1109/MIE.2020.3002486.

[5] M. Schmid, E. Gebauer, and C. Endisch, "Structural analysis in reconfigurable battery systems for active fault diagnosis," *IEEE Trans. Power Electron.*, vol. 36, no. 8, pp. 8672–8684, Aug. 2021, doi: 10.1109/TPEL.2021.3049573.

[6] Z. Zhao, J. Xu, Z. Liu, X. Zhang, and X. Mei, "Reconfigurable battery system-based hybrid self-heating method for low temperature applications," *IEEE Trans. Ind. Informat.*, vol. 20, no. 11, pp. 12826–12836, Nov. 2024, doi: 10.1109/TII.2024.3424564.

[7] S. Lee, G. Noh, and J.-I. Ha, "Reconfigurable power circuits to series or parallel for energy-balanced multicell battery pack," *IEEE Trans. Ind. Electron.*, vol. 70, no. 4, pp. 3641–3651, Apr. 2023, doi: 10.1109/TIE.2022.3181412.

[8] U. Westerhoff, T. Kroker, K. Kurbach, and M. Kurrat, "Electrochemical impedance spectroscopy based estimation of the state of charge of lithium-ion batteries," *J. Energy Storage*, vol. 8, pp. 244–256, Nov. 2016, doi: 10.1016/j.est.2016.09.001.

[9] X. Du, J. Meng, J. Peng, Y. Zhang, T. Liu, and R. Teodorescu, "Sensorless temperature estimation of lithium-ion battery based on broadband impedance measurements," *IEEE Trans. Power Electron.*, vol. 37, no. 9, pp. 10101–10105, Sep. 2022, doi: 10.1109/TPEL.2022.3166170.

[10] Z. Chen, Y. Zhang, C. Liu, R. Yang, and G. Chen, "A novel multisinusoidal PWM excitation for online battery impedance spectroscopy identification and implementation by reconfigurable battery systems," *IEEE Trans. Transport. Electrific.*, vol. 10, no. 4, pp. 8470–8485, Dec. 2024, doi: 10.1109/TTE.2024.3350878.